COBEM 2023 27TH INTERNATIONAL CONGRESS OF MECHANICAL ENGENEERING

ABCM Brazilian Society of Mechanical Sciences and Engineering
27th ABCM International Congress of Mechanical Engineering
December 04-08, 2023, Florianópolis-SC, Brazil

COB-2023-1820
Evaluation of fault detection methodology in roller bearings using time-synchronous average

Racquel Knust Domingues
Júlio Apolinário Cordioli
Federal University of Sanra Catarina, Florianópolis - SC, 88040-900, Brazil
racquel.knust@lva.ufsc.br,julio.cordioli@ufsc.br

Danilo de Souza Braga
Dynamox, Florianópolis - SC, 88030-909, Brazil
danilo@dynamox.net

Abstract. *Proper maintenance is essential in industrial sectors to ensure maximum asset availability and economic return. Predictive maintenance, which is based on monitoring machine conditions, is widely utilized as a strategy. Monitoring the vibrational response of a structure is a key solution for detecting defects and failures in machines and equipment. Vibrational signals from rotating machines typically consist of two components: deterministic and random. The deterministic component is associated with the structural response and operating condition, proving useful in identifying anomalies. The random component can arise from random excitations or electrical noise. Therefore, it is crucial to remove unwanted noise in order to utilize vibration analysis as an effective tool for fault detection. This study proposes an approach based on Time-Synchronous Averaging (TSA) to separate the deterministic and random signals. The methodology employs TSA to extract frequency components related to bearing defects, infering their presence or absence. The study evaluates the effectiveness of the methodology in defect detection and investigates the effects of varying internal parameters of the techniques used, aiming to identify optimal parameters for application in different scenarios.*

Keywords: *Fault Detection, Time-Synchronous Average, Bearing Fault*

1. INTRODUCTION

Predictive maintenance plays a crucial role in ensuring the efficiency and availability of machines. This approach is based on analyzing the current machine conditions to predict failures and perform interventions at the most appropriate time. Unlike corrective and preventive maintenance, predictive maintenance avoids unexpected failures and unnecessary parts replacements, contributing to more agile and efficient production processes (Kardec and Nascif, 2006).

Each component of a machine, as well as any structure, has a specific vibrational response that is directly related to its physical properties or applied excitation. When a failure occurs in a components, there is a direct alteration of the machine or equipment's vibration. This, combined with the fact that vibration measurement is non-intrusive, makes vibration analysis one of the most commonly used techniques in predictive maintenance (Braun *et al.*, 2002).

Generally, when performing vibration measurements on a rotating machine, the obtained signal consists of two main components: a random component and a deterministic component. The random component is related to the noise present in the signal, such as electrical noise from instrumentation or stochastic nature noise, like random slip in bearings. On the other hand, the deterministic component is directly related to the machine's structure and operating conditions. This is the part of the signal that needs to be analyzed to detect the presence of a fault. Therefore, during vibration analysis, it is important to identify and separate the deterministic component of the signal to enable a precise assessment of the machine's condition and detect possible faults (Randall, 2021).

A traditional and straightforward method for separating the deterministic components from the random components is the Time-Synchronous Average (TSA). This method involves calculating the average of signal segments that are related to a specific frequency. This averaging process corresponds to a frequency-domain filtering operation, which has the characteristic of attenuating components unrelated to the synchronization frequency, resulting in the separation of the component at that frequency and its harmonics (Hochmann and Sadok, 2004).

Although TSA is a simple technique, its application is limited under certain operating conditions, such as when the analyzed signal varies with rotation. In these situations, a common approach is order analysis, which involves transforming the signal's time domain analysis into the angular domain. This way, the analysis is conducted with respect to rotation, regardless of the time interval associated with that rotation. This allows for segment averaging, even when fluctuations in rotation speed occur. Angular resampling is a numerical technique that facilitates the application of order analysis, using reference information about the phase of the axis (Fyfe and Munck, 1997). This information can be obtained through an

external device, such as a tachometer, or through rotation estimation techniques based on vibration.

Therefore, this study aims to evaluate a methodology for detecting faults in rolling bearings, considering the use of TSA to extract the deterministic components related to characteristic fault frequencies. The main proposal of the methodology is to extract these components associated with the fault frequencies and assess their magnitudes for defect detection. The adopted workflow involves obtaining experimental data, signal processing to extract relevant information, and finally, performing fault detection.

2. THEORETICAL FOUNDATION

Fault detection in machines is achieved by comparing the signal under analysis with an established pattern. There are various approaches to perform this comparison, as well as different criteria to determine whether the signal indicates a fault in a component. One simple way to make this comparison is by evaluating vibration levels. By using vibration criteria, which are measures that establish acceptable limits of vibration for proper machine operation, it is possible to verify if the measured vibration levels fall within these limits. Another approach is spectral analysis. Since the vibrational responses of mechanical elements with faults have characteristic frequencies, analyzing the signal in the frequency domain allows for the identification of a fault by comparing the magnitude values of the components at these specific frequencies with established patterns (Randall, 2021).

In this section, we will address some fundamental concepts necessary for understanding the fault detection methodology evaluated in this study. Firstly, we will describe how vibrational signals from rolling bearings are characterized under faulty operating conditions. Then, we will present the fundamentals of signal processing techniques used in the methodology.

2.1 Vibratory Signals in Rolling Bearings

Rolling bearings are components designed to support loads and serve as supports for rotating shafts. In general, bearings can exhibit localized defects in their components, such as the outer ring, inner ring, and rolling elements, due to fatigue, resulting in cracks or cavities. When a collision occurs between such a defect and the bearing surfaces, an impact is generated in the bearing and, consequently, in the machine. This impact can be modeled as an impulse applied to the system, resulting in the dynamic excitation of the bearing and the machine. As a result, when a sensor is attached at a fixed point on the defective bearing, the measured vibration represents the impulsive response of the system at that point. Due to the rotation of the bearing and the movement of the shaft, this impulse is generated periodically, resulting in a sequence of impulsive responses. When the defect is located in the rings, an impact occurs each time a rolling element collides with them. On the other hand, when the defect is in the rolling elements, an impact occurs each time the defect collides with the rings. By knowing the rotational frequency of the shaft, f_r, and the bearing geometry, it is possible to calculate the frequency of occurrence of these impulsive responses according to the defect's location (Utpat *et al.*, 2009). These frequencies are known as defect frequencies and are defined as follows:

$$f_e = \frac{nf_r}{2}\left\{1 - \frac{d}{D}\cos\phi\right\}, \quad f_i = \frac{nf_r}{2}\left\{1 + \frac{d}{D}\cos\phi\right\}, \quad f_{er} = \frac{f_r D}{d}\left\{1 - \left(\frac{d}{D}\cos\phi\right)^2\right\}, \tag{1}$$

where f_e is the outer ring defect frequency, f_i is the inner ring defect frequency, and f_{er} is the rolling element defect frequency. The internal parameters in these definitions are D, which is the pitch diameter of the bearing, d, which is the diameter of the rolling element, ϕ, which is the contact angle relative to the radial plane, and n, which is the number of rolling elements. Another important frequency in bearing analysis is the cage frequency, f_g, which represents the frequency at which the cage rotates around its own axis and can be defined as follows:

$$f_g = \frac{f_r}{2}\left\{1 - \frac{d}{D}\cos\phi\right\}. \tag{2}$$

Another characteristic present in the response to these types of defects is amplitude modulation, which occurs due to two main factors. The first factor is related to the modulation of the impulse intensity generated, influenced by the non-uniform load distribution in the bearing housing. The second factor arises from variations in the transfer function, which determines the path of energy propagation generated by the impulses, due to the presence of a fixed ring and other moving elements. This variation occurs with respect to the fixed sensor position (Sawalhi *et al.*, 2007). In Fig. 1 presents the expected signals for bearing defects in the outer ring, inner ring, and rolling elements, along with the signals that modulate the sequence of impulsive response for each defect.

2.2 Envelope Analysis

One widely used technique for fault detection in rolling bearings is envelope analysis. This technique is motivated by the occurrence of random fluctuations in the occurrence frequency of impulses, resulting from variations in the contact

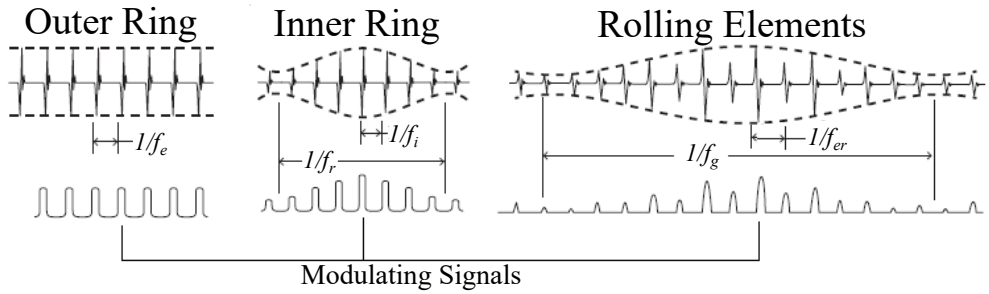

Figure 1. Signals of Bearing Defects (Adapted from Randall (2021))

angle (ϕ) with each passage of the rolling elements through the load distribution zone. Although this fluctuation is small and almost imperceptible in the time domain signal, its effect on the spectrum can cause lateral spreading of frequency components and, consequently, unwanted overlaps (Ho and Randall, 2000).

Envelope analysis employs a methodology that exclusively extracts information related to the amplitude modulation of the signal. This procedure involves three main steps. In the first step, a region in the signal's spectrum is identified where a possible natural frequency of the system exists, which is presumably directly related to the response to impulses generated by the defect. The signal is then filtered within this frequency range, removing all other components and isolating only the sequences of impulse responses. In the second step, the modulating signal is extracted from the filtered signal using Hilbert transform demodulation. The final step in envelope analysis is obtaining a spectrum of the envelope signal. If the analyzed signal originates from a bearing with a defect, this spectrum will have components associated with defect frequencies, as the modulating signals exhibit periodicity related to these frequencies (Randall, 2021).

2.3 Time-Synchronous Averaging

Time-Synchronous Averaging (TSA) not only separates the deterministic part of the signal from the random part but also has the ability to isolate components at specific frequencies, justifying the term 'Synchronous' in its name (Randall *et al.*, 2011). To understand the application of this technique, it can be defined that a time signal, $x(t)$, can be decomposed into three distinct components. The first is the deterministic and synchronous component at the desired frequency f_s to isolate, $s(t)$, the second is the deterministic and non-synchronous component, $n(t)$, and the third is the random component of the signal, $r(t)$.

Therefore, to extract the component $s(t)$ through Time Synchronous Averaging (TSA), it is sufficient to apply a transformation to $x(t)$ using the average of segments of this signal, with intervals equivalent to the period T_s (=$1/f_s$). In each segment, the synchronous component $s(t)$ will have similar shapes due to its periodicity, while the other components will exhibit disordered behaviors. This occurs because the portion $r(t)$ has random characteristics, resulting in random samples in each segment, and the portion $n(t)$ is out of sync with the segment interval, resulting in different parts of this component in each segment (Ha *et al.*, 2016). Taking these aspects into consideration, at the end of the segment averaging process, the values of the component $s(t)$ will remain close to their original values, while the other components may tend to be attenuated, as can be observed in Fig. 2.

Mathematically, this process of averaging over N segments can be formulated as a convolution of the signal $x(t)$ with a sequence of N ideal impulses spaced by T_s and with amplitudes equal to $1/N$, resulting in $y(t)$. Due to the property of convolution in the Fourier transform domain, this model can be represented in the frequency domain through multiplication, as follows:

$$Y(f) = X(f)C(f) = X(f)\frac{1}{N}\frac{sen(\pi N T_s f)}{sen(\pi T_s f)}, \tag{3}$$

where f is the frequency variable, j is the imaginary unit, $X(f)$ is the Fourier transform of the signal $x(t)$, and $C(f)$ is the Fourier transform of the impulse sequence. It can be observed that multiplication in the frequency domain is analogous to filtering, where $C(f)$ is defined as the filter response. Its definition indicates that $|C(f)|$ resembles a sequence of peaks centered at multiples of f_s, equally spaced. Therefore, by performing the multiplication in the frequency domain, as described in Eq. 3, we can understand the extraction process through TSA (Braun, 1975).

2.4 Order Analysis and Angular Resampling

Although TSA is a relatively straightforward technique, its effectiveness relies on having an equal number of samples in each segment corresponding to the interval T_s. However, it is common for this equality to be compromised due to

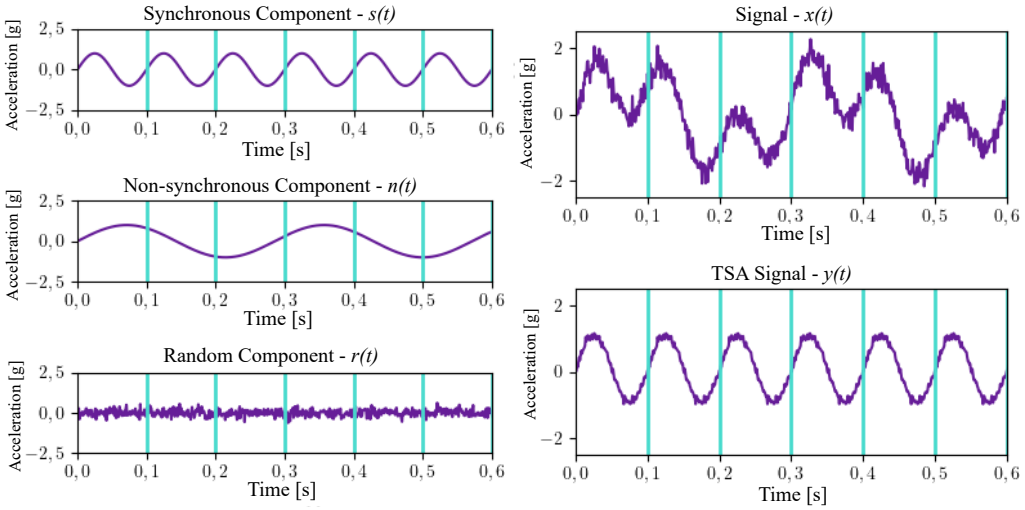

Figure 2. Constituent Components of a Signal and Result of TSA Application

various factors. To address this issue, it is possible to manipulate the signal so that it is analyzed with respect to a specific frequency and its harmonics, referred to as orders. In the case of analyzing signals based on the rotation of a shaft, this process must ensure that the same number of samples of the signal is obtained for each rotation, which means that the sampling should be performed with equal angular increments. In this way, even if there are fluctuations in the rotational frequency, the spectral information remains comprehensible because it is related to the rotation itself and not to an absolute value (Borghesani *et al.*, 2014).

To perform this transformation, angular resampling was used. This approach consists of three steps. In the first step, the time instants at which a complete rotation of the shaft occurs, known as rotation periods, are determined. These moments are identified using an external signal, often generated by a tachometer. The second step involves determining the moments at which regular angular increments occur by using numerical interpolation and the instants obtained in the previous step to obtain a function that describes the relationship between time and angle, $t(\Theta)$. The third step involves resampling the signal in the angular domain using the times associated with the regular angular increments obtained in the previous step (Fyfe and Munck, 1997).

2.5 Estimation of Rotation through Vibration

Obtaining a synchronization signal, which contains the rotational speed information, through an external device like a tachometer can be impractical in certain industrial applications. Therefore, the use of techniques to estimate the rotational speed of a machine based on its own vibration can provide a solution to this problem (Schmidt *et al.*, 2018). In this work, three methodologies were used to estimate the rotational frequency: phase demodulation (Bonnardot *et al.*, 2005), maximum spectrogram tracking (Urbanek *et al.*, 2011), and a combination of the two approaches to achieve an improved final result (Urbanek *et al.*, 2013).

Phase demodulation is based on separating and processing specific components of the signal that are directly associated with the shaft frequency and extracting phase-related information about the shaft rotation, which, in turn, is directly related to its rotational speed. The first step involves identifying this component. Then, it needs to be separated from the original signal for further processing. This can be achieved by applying a band-pass filter. It is important to choose an appropriate bandwidth for the filter to extract only the desired component. With the filtered signal, the Hilbert transform is applied to this component to obtain the phase over time. This extracted phase information can be used to determine the time instants associated with shaft revolutions, which are used in angular resampling. It should be noted that a complete rotation corresponds to an increase of 2π in the shaft's phase (Bonnardot *et al.*, 2005).

Maximum spectrogram tracking is based on using the spectrogram to identify, at each time instant, which frequencies have the highest energy within a specific range. With this, a maximum frequency function in time can be constructed, and it is assumed that this corresponds to the instantaneous frequency of the axis. From the tracked maximum frequency function, f_{max} obtained by the method, it is possible to calculate the associated instantaneous phase, θ_{max}, in the following manner:

$$\theta_{max}(t) = 2\pi \int_0^t f_{max}(u)du. \tag{4}$$

Once the shaft phase is obtained, it can be used to extract the time instants associated with shaft revolutions, similar to what is done in phase demodulation, and utilize them in angular resampling (Urbanek *et al.*, 2013).

The hybrid method is a combination of the two previous methods. First, maximum spectrogram tracking is used to perform a preliminary angular resampling. After this step, any type of smearing is removed from the signal, and frequency components are represented by peaks in the orders. This allows for the use of a narrow filter centered on the order in the resulting signal from the first process. Next, the filtered signal is reversed to the time domain through inverse resampling. With the filtered signal in the time domain, phase demodulation can be applied to obtain the final estimation of the shaft rotation (Urbanek *et al.*, 2011).

3. MATERIALS AND METHODS

The methodology employed in this study for bearing fault detection is divided into three main stages, as illustrated in the flowchart presented in Fig. 3. This approach follows a well-established pattern in condition monitoring for fault detection in machine elements, where a vibratory signal is measured and processed to extract relevant information that indicates the presence or absence of faults in the analyzed element (Jin *et al.*, 2009).

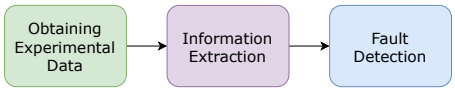

Figure 3. General Flowchart of Applied Methodology for Failure Detection

The first stage is data acquisition. In this study, the data was generated through a machine fault simulation test bench manufactured by SpectraQuest, as shown in Fig. 4. The main system of the test bench consists of a motor driven by a frequency inverter, allowing user control of the speed. The motor is connected to a shaft supported by two bearing housings. At the end of the shaft farthest from the motor, there is a pulley that, through a belt system, is connected to a larger pulley, which, in turn, is linked to a gearbox. This gearbox is responsible for transmitting torque from a magnetic brake to the previously mentioned system. The magnetic brake's purpose is to generate a load on the system.

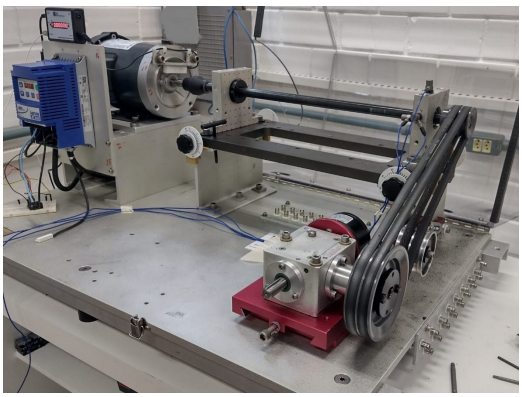

Figure 4. Fault Simulation Test Bench

A test matrix was established with seven different operating conditions, grouped into five distinct classes and their variations, as presented in Table 1. These conditions pertain to the rotational speed of the shaft and the configuration of the main system of the test bench. A test matrix was created for each fault condition (healthy, outer race, inner race, and rolling element) with a shaft rotational speed of 1200 RPM.

Table 1. Bench operating conditions

Classe	Variação	Descrição
A	-	Constant speed and no load
B	a	Speed varying by 1% and no load
B	b	Speed varying by 5% and no load
B	c	Speed varying by 10% and no load
C	-	Constant speed, no load and with shaker attached
D	a	Constant speed and 50% load
D	b	Constant speed and 100% load

Three PCB accelerometers, model 353C33, were used, mounted perpendicular to each other to simulate a triaxial sensor at a single point. In addition to the signals from these three accelerometers, simultaneous acquisition of the test bench's integrated tachometer was also performed. All signals were measured with an acquisition time of 30 seconds and a sampling frequency of 25600 samples per second using a National Instruments acquisition module, model 9234.

Two general sets of data were generated, each containing 28 subsets of signals (acceleration and tachometer data), which are divided into 4 groups, each with 7 subsets of signals corresponding to the 7 proposed operating conditions. Each group corresponds to a bearing fault condition. The creation of two general sets of data is necessary due to the methodology applied for fault detection, as an optimization process will be used. It requires one set for training the optimization and another for testing it.

The second stage corresponds to the purple-highlighted block in the flowchart presented in Fig. 3. In this block, the experimental data obtained in the previous stage is processed to extract relevant information for fault detection. In this study, a processing methodology is employed that involves applying envelope analysis to the signal, followed by angular resampling and time-synchronous averaging, synchronized with the characteristic fault frequencies mentioned in Eq. 1. The flowchart of this information extraction methodology is presented in Fig. 5.

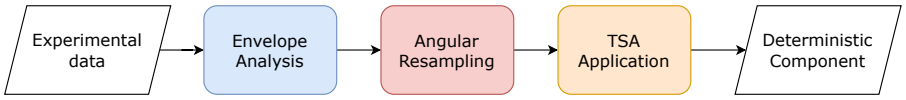

Figure 5. Information Extraction Methodology Flowchart

The processing begins with the application of envelope analysis. In this work, a predefined filtering band from 500 Hz to 10 kHz was used, as the objective is to evaluate the other processing steps and not to focus on the envelope analysis performance. Next, angular resampling is applied, for which it was necessary to obtain the times corresponding to the intervals related to the extraction frequencies. These times were obtained using either the tachometer or rotation estimation techniques. In the case of the tachometer, a rising edge detection algorithm was used to obtain the rotation frequency, and, using the relationships presented in Eq. 1, the defect frequencies were obtained. When rotation estimation techniques were employed, the expected defect frequencies themselves were used as a reference component in demodulation and as a starting point for tracking the maximum in the spectrogram and for the hybrid method.

Rotation estimation techniques share a common parameter in their applications. Both in the phase demodulation filtering process and in the search for the maximum frequency at each instant of the spectrogram maximum tracking (also present in the first block of the hybrid method), it is necessary to determine a frequency range for analysis. In this work, four different values for this frequency range were explored. Considering that f_c represents the central value of the range, the frequency analysis range is $f_c \pm \delta f_c$, where δf_c is defined as βf_c. The parameter β represents the percentages used, which were defined as 1,25 %, 2 %, 5 %, 10 % and 15 %. These values were defined by the authors to evaluate the behavior of the methods for different input parameters, considering the diversity of signals used in this work.

The signals were evaluated in three directions measured in the bearing under analysis (vertical, horizontal, and axial) for use in the rotation estimation techniques. For each direction, the five proposed frequency range values were explored. An algorithm was used to select the combination of direction and range that resulted in the lowest error in each technique. The error was assessed using the mean relative percentage error of the frequency obtained in each technique, with the tachometer used as the reference.

With the resampled signal, the final step of the flowchart presented in Fig. 5, highlighted in orange, can be applied. The segmentation required for the application of time-synchronous averaging (TSA) was performed considering that the number of samples per revolution is known, as it was defined during the angular resampling. It is important to note that in this work, the choice was made to use as many segments as possible within the signal, meaning the total number of rotations that occurred during the signal acquisition time was considered. This way, all available segments were used to calculate the average.

For the blue-highlighted block in the flowchart shown in Fig. 3, a detection algorithm was employed. This algorithm compares the magnitudes of the fault frequency harmonics with a predetermined threshold and determines the presence of a fault if at least two out of the three magnitude values exceed the thresholds. The fault detection is determined based on the following criteria:

$$C_1 : A_1 \geq l_1, \quad C_2 : A_2 \geq l_2, \quad C_3 : A_3 \geq l_3, \tag{5}$$

$$N(C_1, C_2, C_3) \geq 2 \Rightarrow DEFECT, \quad N(C_1, C_2, C_3) < 2 \Rightarrow NO\ DEFECT, \tag{6}$$

where A_1, A_2, and A_3 represent the magnitudes of the first three harmonics of the fault frequency in the analyzed signal, l_1, l_2, and l_3 are the pre-defined thresholds, C_1, C_2, and C_3 are the magnitude comparisons, $N()$ indicates the count of true comparisons, and the indices 1, 2, and 3 refer to the harmonics.

These thresholds are determined by multiplying coefficients by the magnitudes of the fault frequency harmonics obtained from a vibration signal of a healthy bearing. Separate thresholds are defined for each harmonic, allowing for a more precise analysis. The purpose of defining the thresholds through this multiplication is to determine at what deviation from normality a fault can be identified. Therefore, the thresholds can be defined as follows:

$$l_1 = c_1 N_1, \quad l_2 = c_2 N_2, \quad l_3 = c_3 N_3, \tag{7}$$

where c_1, c_2, and c_3 are the coefficients and N_1, N_2, and N_3 are the normal values.

The coefficients were determined through an optimization of balanced accuracy (BA), which is defined as follows:

$$BA = \frac{1}{2}\left(\frac{TP}{TP+FN} + \frac{TN}{TN+FP}\right) \tag{8}$$

where TP is the number of true positives, TN is the number of true negatives, FP is the number of false positives, and FN is the number of false negatives. These parameters reflect the performance of the detection. A true positive occurs when the algorithm correctly detects a fault in a signal from a defective component. A false positive occurs when the algorithm incorrectly detects a fault in a signal from a non-defective component. Similarly, a true negative occurs when the algorithm correctly does not detect a fault in a signal from a non-defective component. A false negative occurs when the algorithm fails to detect a fault in a signal from a defective component. In this step, the training dataset was used to obtain the coefficients.

4. RESULTS AND DISCUSSION

In order to evaluate the performance of the rotation estimation techniques, the vibration signals from the bearing without any faults were used to estimate the shaft rotation frequency. This choice was motivated by the fact that the tachometer provides direct information about the shaft rotation, serving as a precise reference for error calculation. Errors were calculated for all 15 possible combinations (3 accelerometer directions x 5 frequency analysis ranges). Table 2 presents the minimum error obtained for each operating condition (OC), along with the corresponding technique, frequency range, and accelerometer direction that produced it.

Table 2. Minor Errors - Rotation Estimation Techniques

	A	**Ba**	**Bb**	**Bc**	**C**	**Da**	**Db**
Technique	Phase Demodulation	Phase Demodulation	Phase Demodulation	Phase Demodulation	Spectrogram Tracking	Phase Demodulation	Spectrogram Tracking
Direction	Horizontal	Horizontal	Horizontal	Horizontal	Vertical	Axial	Vertical
Range	1.25 %	10 %	15 %	15 %	1.25 %	1.25 %	1.25 %
Error	0.037 %	0.135 %	0.292 %	0.566 %	0.047 %	0.326 %	0.275 %

The results regarding the direction were expected, as the vertical and horizontal directions correspond to the radial directions where the vibration induced by any unbalance will be more pronounced. Regarding the frequency range, it can be observed that in cases of constant rotation, a narrow range enables the extraction of only the rotation component, preventing information from other components from contaminating the estimation of the technique. On the other hand, in cases where there is rotational variation, the frequency range should be appropriate to capture this variation, encompassing the entire range where frequency spreading occurs.

The proposed fault detection methodology in this study was evaluated in stages to examine the impact of each stage on the detection process. Three detection processes were conducted: (1) involved the application of envelope analysis alone on the signals, (2) was performed after the execution of envelope analysis and angular resampling, and (3) was carried out by applying the complete methodology, including envelope analysis, angular resampling, and time-synchronous averaging.

The balanced accuracies of each detection process obtained from the test set will be presented. It is important to note that for the second and third detection processes mentioned earlier, the results are evaluated for each rotation estimation technique (phase demodulation, maximum spectrogram tracking, and the hybrid method), as well as for the tachometer. Tables 3 to 5 present the obtained values of balanced accuracies for the detection of faults in the outer ring, inner ring, and rolling elements, respectively.

Table 3. Balanced Accuracies - Outer Ring - Test

	Vertical			**Horizontal**			**Axial**		
Detection Process	**(1)**	**(2)**	**(3)**	**(1)**	**(2)**	**(3)**	**(1)**	**(2)**	**(3)**
-	0.74	-	-	0.74	-	-	0.52	-	-
Tachometer	-	0.88	0.83	-	0.83	0.81	-	0.86	0.86
Demodulation	-	0.86	0.83	-	0.88	0.79	-	0.90	0.86
Spectrogram	-	0.93	0.93	-	0.88	0.83	-	0.71	0.62
Hybrid	-	0.83	0.80	-	0.74	0.76	-	0.79	0.76

Several observations can be made regarding these results. Firstly, it is noticeable that the values obtained for defect detection in the rolling elements were significantly lower compared to the values of the other detections. This can be attributed to the behavior of these signals, as they did not exhibit defect-related components prominently. Furthermore,

Table 4. Balanced Accuracies - Inner Ring - Test

	Vertical			Horizontal			Axial		
Detection Process	**(1)**	**(2)**	**(3)**	**(1)**	**(2)**	**(3)**	**(1)**	**(2)**	**(3)**
-	0.90	-	-	1.00	-	-	0.71	-	-
Tachometer	-	1.00	0.93	-	0.98	1.00	-	0.93	0.93
Demodulation	-	0.88	0.95	-	0.98	0.95	-	0.83	0.79
Spectrogram	-	0.90	0.88	-	1.00	0.93	-	0.93	0.95
Hybrid	-	0.88	0.98	-	0.98	1.00	-	0.93	1.00

Table 5. Balanced Accuracies - Rolling Elements - Test

	Vertical			Horizontal			Axial		
Detection Process	**(1)**	**(2)**	**(3)**	**(1)**	**(2)**	**(3)**	**(1)**	**(2)**	**(3)**
-	0.36	-	-	0.5	-	-	0.64	-	-
Tachometer	-	0.52	0.69	-	0.52	0.52	-	0.76	0.81
Demodulation	-	0.48	0.45	-	0.57	0.45	-	0.64	0.55
Spectrogram	-	0.48	0.5	-	0.52	0.52	-	0.71	0.71
Hybrid	-	0.43	0.48	-	0.38	0.57	-	0.64	0.62

it is noted that defect detection in the inner race showed better results. This may be related to the fact that signals from this defect displayed more prominent harmonics at the defect frequency. To illustrate this, Fig. 6 displays the spectra of the faulty signal and the reference signal for the outer race, inner race, and rolling element defects, respectively, under the Db operating condition (with 100 % load). It is evident that the difference in magnitude at the defect frequency and its harmonics, highlighted in green, is significantly greater for the signal with an inner race defect.

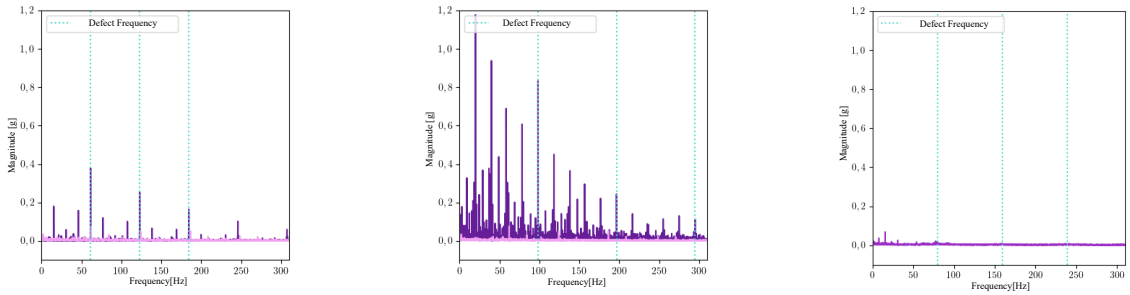

a) Outer Ring Defect b) Inner Ring Defect b) Rolling Elements Defect

Figure 6. Order Spectra - Defective Bearing and Healthy Bearing - Cond. Op.: Db

It's also important to note that the second detection process (2), which involves angular resampling, showed an improvement in detection in 70 % of the cases compared to the first process (1). This can be directly attributed to angular resampling, which avoids potential errors caused by the fluctuation of this frequency. To illustrate this behavior, let's use the example of the vertical accelerometer signal measured on a bearing with an outer race defect in the Bc operating condition (RPM varying by 15 %). In Fig. 7 displays the spectrum of the envelope signal along with the envelope spectrum of the reference signal (without a defect). It can be observed that the defect-related components show slight dispersion due to the rotation variation. On the other hand, Fig. 8 presents the order spectrum of the resampled defective signal, along with the order spectrum of the resampled reference signal. In this spectrum, it is noticeable that the defect-related components, along with other components of the spectrum, no longer exhibit frequency dispersion and are now seen as peaks centered on their respective orders, making fault detection easier.

Regarding the application of the third detection process (3), which encompasses the entire proposed methodology, it was observed that the results obtained, in the vast majority of cases, were better than those obtained in the first detection process (1). However, there was no significant improvement in results compared to the second detection process (2), with some cases showing maintained balanced accuracy and others experiencing a slight decrease. It is presumed that the motivation behind these results lies in the behavior of the analyzed signals since, in many cases, the defect-related component was already well-characterized with angular resampling alone. To illustrate, in Fig. 9, the order spectrum of the signal resulting from TSA with a defect is shown along with the order spectrum of the reference TSA signal from the previous example. It is clear that TSA demonstrates efficiency by displaying only the components related to the defect in the spectrum. However, it can be noticed that these components were already highlighted with just angular resampling, as shown in Fig. 8.

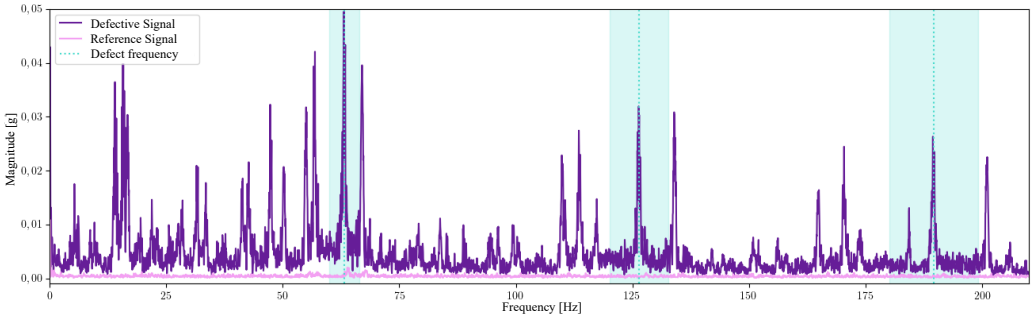

Figure 7. Envelope Signal Spectra - Vertical - Cond. Op.: Bc - Outer Ring Defect/Reference

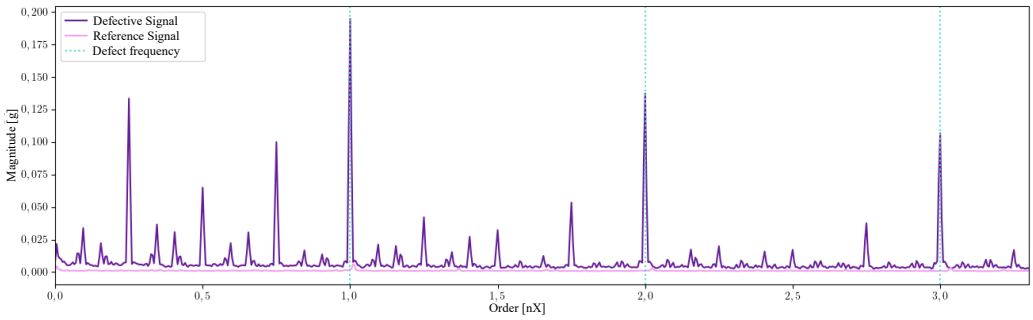

Figure 8. Resampled Signal Spectra - Vertical - Cond. Op.: Bc - Outer Ring Defect/Reference

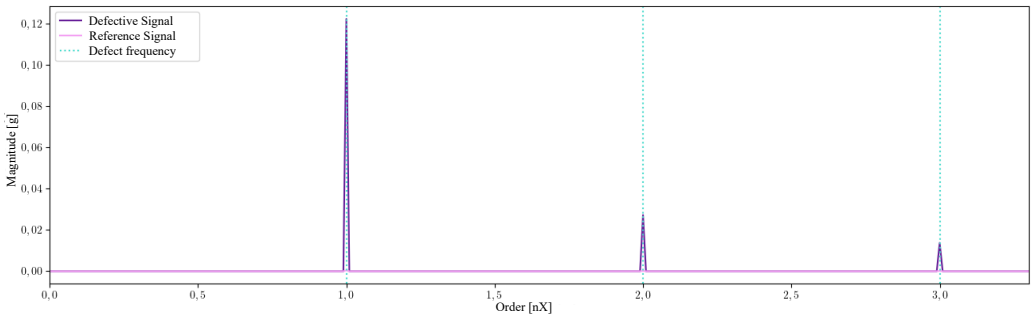

Figure 9. TSA Signal Spectra - Vertical - Cond. Op.: Bc - Outer Ring Defect/Reference

5. CONCLUSIONS

In this study, a methodology for detecting defects in bearing housings was analyzed, involving signal processing techniques such as envelope analysis, angular resampling, and time synchronous averaging. Envelope analysis extracts specific defect-related information, while angular resampling deals with speed variations, and time synchronous averaging separates the deterministic defect frequency components. Two approaches were considered to obtain synchronization signals in angular resampling, using the tachometer signal or frequency estimation techniques. Three frequency estimation techniques were evaluated (phase demodulation, spectrogram peak tracking, and hybrid method), demonstrating that signals from the vertical and horizontal accelerometers showed lower estimation error, and the frequency range should be adjusted to cover the shaft speed variations.

The step-by-step evaluation of the proposed methodology for fault detection revealed some important points. It was observed that the application of angular resampling was a crucial step to improve detection results. Analysis in the order domain allowed for a more precise assessment of defect-related components, which contributed to better detection performance. The application of time synchronous averaging (TSA) did not show a significant improvement in results, suggesting that angular resampling alone was sufficient to obtain good results in the detection of the analyzed signals.

Therefore, this work concludes that the proposed methodology can be effective for bearing fault detection, although some considerations must be taken into account. The first one pertains to the choice between using the tachometer or frequency estimation techniques. While the tachometer showed superior results, these techniques proved promising in cases where the frequency-related component under analysis is well-characterized in the spectrum, i.e., has a high SNR. Angular resampling emerged as a fundamental tool to handle signals with varying rotation, and TSA demonstrated its ability to extract synchronous components, particularly when the synchronization frequency is well-defined.

6. ACKNOWLEDGEMENTS

We thank Dynamox S/A and the Laboratory of Vibrations and Acoustics at UFSC, supported by FEESC, for making this work possible through the project "Technologies for the analysis of noise and vibration signals for the detection, prognosis, and correction of failures in machines and structures."

7. REFERENCES

Bonnardot, F., El Badaoui, M., Randall, R., Danière, J. and Guillet, F., 2005. "Use of the acceleration signal of a gearbox in order to perform angular resampling (with limited speed fluctuation)". *Mechanical Systems and Signal Processing*, Vol. 19, No. 4, pp. 766–785. ISSN 0888-3270.

Borghesani, P., Pennacchi, P., Chatterton, S. and Ricci, R., 2014. "The velocity synchronous discrete fourier transform for order tracking in the field of rotating machinery". *Mechanical Systems and Signal Processing*, Vol. 44, No. 1-2, pp. 118–133.

Braun, S., Ewins, D., Rao, S.S. and Leissa, A., 2002. "Encyclopedia of vibration: Volumes 1, 2, and 3". *Appl. Mech. Rev.*, Vol. 55, No. 3, pp. B45–B45.

Braun, S., 1975. "The extraction of periodic waveforms by time domain averaging". *Acta Acustica united with Acustica*, Vol. 32, No. 2, pp. 69–77.

Fyfe, K. and Munck, E., 1997. "Analysis of computed order tracking". *Mechanical systems and signal processing*, Vol. 11, No. 2, pp. 187–205.

Ha, J.M., Youn, B.D., Oh, H., Han, B., Jung, Y. and Park, J., 2016. "Autocorrelation-based time synchronous averaging for condition monitoring of planetary gearboxes in wind turbines". *Mechanical Systems and Signal Processing*, Vol. 70, pp. 161–175.

Ho, D. and Randall, R., 2000. "Optimisation of bearing diagnostic techniques using simulated and actual bearing fault signals". *Mechanical systems and signal processing*, Vol. 14, No. 5, pp. 763–788.

Hochmann, D. and Sadok, M., 2004. "Theory of synchronous averaging/sup/spl omega". In *2004 IEEE Aerospace Conference Proceedings (IEEE Cat. No. 04TH8720)*. IEEE, Vol. 6, pp. 3636–3653.

Jin, G., Xiang, Z. and Lv, F., 2009. "Semantic integrated condition monitoring and maintenance of complex system". In *2009 16th International Conference on Industrial Engineering and Engineering Management*. IEEE, pp. 670–674.

Kardec, A. and Nascif, J., 2006. "Manutenção: função estratégica rio de janeiro: Qualitymark, 2006".

Randall, R., Sawalhi, N. and Coats, M., 2011. "A comparison of methods for separation of deterministic and random signals". *International Journal of Condition Monitoring*, Vol. 1, No. 1, pp. 11–19.

Randall, R.B., 2021. *Vibration-based condition monitoring: industrial, automotive and aerospace applications*. John Wiley & Sons.

Sawalhi, N., Randall, R. and Endo, H., 2007. "The enhancement of fault detection and diagnosis in rolling element bearings using minimum entropy deconvolution combined with spectral kurtosis". *Mechanical Systems and Signal Processing*, Vol. 21, No. 6, pp. 2616–2633.

Schmidt, S., Heyns, P.S. and De Villiers, J.P., 2018. "A tacholess order tracking methodology based on a probabilistic approach to incorporate angular acceleration information into the maxima tracking process". *Mechanical Systems and Signal Processing*, Vol. 100, pp. 630–646.

Urbanek, J., Barszcz, T. and Antoni, J., 2013. "A two-step procedure for estimation of instantaneous rotational speed with large fluctuations". *Mechanical Systems and Signal Processing*, Vol. 38, No. 1, pp. 96–102.

Urbanek, J., Barszcz, T., Sawalhi, N. and Randall, R.B., 2011. "Comparison of amplitude-based and phase-based method for speed tracking in application to wind turbines". *Metrology and measurement systems*, Vol. 18, No. 2, pp. 295–303.

Utpat, A., Ingle, R. and Nandgaonkar, M., 2009. "A model for study of the defects in rolling element bearings at higher speed by vibration signature analysis". *World Academy of Science, Engineering and Technology*, Vol. 56, pp. 130–136.

8. RESPONSIBILITY NOTICE

The authors are solely responsible for the printed material included in this paper.